Standoff Raman spectroscopy for architectural interiors from 3-15 m distances

Yu Li, Chi Shing Cheung, Sotiria Kogou, Florence Liggins, and Haida Liang[*] (iD)

School of Science & Technology, Nottingham Trent University, Nottingham NG11 8NS, UK
[*]*haida.liang@ntu.ac.uk*

Abstract: Portable and mobile Raman spectroscopy systems are increasingly being adopted in *in situ* non-invasive examination of artworks given their high specificity in material identification. However, these systems typically operate within centimeter range working distances, making the examination of large architectural interiors such as wall paintings in churches challenging. We demonstrate the first standoff Raman spectroscopy system for *in situ* investigation of historic architectural interior at distances > 3 m. The 780 nm continuous wave laser-induced standoff Raman system was successfully deployed for the *in situ* examination of wall paintings, at distances of 3–15 m, under ambient light. It is able to identify most common pigments while maintaining a very low laser intensity to avoid light induced degradation. It is shown to complement our current method of standoff remote surveys of wall paintings using spectral imaging.

1. Introduction

The identification of materials such as pigments plays an important role in the study of wall paintings in caves, tombs and buildings since they can reveal information about art history, trade and cultural exchanges in the past, as well as monitoring signs of degradation. However, these paintings are fragile, which limits the possibilities of sampling or contact measurements, and therefore necessitates *in situ* and non-invasive measurements. Some challenges specific to wall paintings may arise from the remoteness of the sites, the inaccessible height of the paintings and the difficulty in controlling the environment they are in. Traditionally, the inspection of upper parts of a wall or ceiling needs scaffolding, which is costly, inconvenient and unstable for sensitive measurements that require long acquisition time [1].

One of the solutions addressing these issues is a visible/near infrared remote spectral imaging system, PRISMS, developed in our group with the ability to image wall paintings at sub-millimeter resolutions from a distance of tens of meters [2]. However, reflectance spectroscopy alone is sometimes not sufficient to give definitive identification of pigments. Therefore, a standoff Raman system is needed as a complementary technique.

Raman spectroscopy is capable of giving very specific material identifications by observing the sharp Raman lines, which provide information about the molecular structure of the material. With the development of powerful laser sources and sensitive detectors in the last three decades, it has become one of the commonly used methods in the field of cultural heritage research for non-invasive material identification (e.g. pigments of paintings), diagnosis of art works (e.g. the extent of degradation), provenance determination, etc. [3–7]. However, limitations include the presence of fluorescence that could potentially mask the Raman signal, and the potential laser-induced degradation that limits the incident laser intensity.

In this paper, we define standoff Raman systems as instruments that can work at distances greater than 3 m and less than 50 m between instrument and object. The idea of performing Raman measurements remotely emerged in the 1960s in atmospheric scattering experiments [8,9].

Currently, most standoff and remote Raman systems have been applied to planetary science and explosive detection, employing high-power pulsed laser sources [10]. However, laser-induced degradation must be taken into careful consideration in the field of cultural heritage research. The intensity and fluence of the laser need to be strictly controlled in Raman measurements to avoid damaging the artworks.

In this paper, we present the developments of a mobile standoff Raman system for wall paintings working in the range from 3 to 15 m using a continuous wave (CW) laser at 780 nm, and its first application in remote pigment identifications of wall paintings.

2.   A remote Raman system for architectural interiors

The standoff Raman spectroscopy system for architectural interiors including wall paintings is designed to satisfy the following requirements: 1) it must be sensitive enough to be able to detect and identify most common historic artist pigments from a distance of 4 m at a spectral resolution of ~8 cm^{-1} in 30 mins; 2) laser intensity must be safe for all pigments; 3) it must be mobile to allow for *in situ* measurements; 4) it must be able to operate under daylight conditions, since it is not always possible to gain access at night; 5) laser excitation beam needs to be co-axial with the collection optics such that the alignment between the excitation and collection beams is distance independent; 6) the laser spot should be < 10 mm in diameter at a distance of 10 m; 7) precise measurement location must be recorded online.

The schematics of a standoff Raman system developed for working at distances > 3 m is shown in Fig. 1(a). The laser beam is reflected by two mirrors placed at 45° such that the laser beam is co-axial with the telescope's axis. The instrument employs a CW laser source for excitation at 780 nm (Newport TLB-7113-01, a temperature stabilized external cavity diode laser with a maximum output power of 90 mW and tuning range from 765 nm to 782 nm), a telescope (Meade ETX-90, a Maksutov-Cassegrain reflector with 90 mm clear aperture and 1250 mm focal length), and an Andor Shamrock spectrograph equipped with a high sensitivity Andor iDus CCD detector thermoelectrically cooled to −75°C. The output laser beam is collimated with a slight divergence which results in a spot diameter on the target of ~4 mm at 3 m and ~8 mm at 8 m. A bandpass filter centred at 780 nm with a FWHM bandwidth of ~3 nm was used to clean-up the laser beam. The scattered and reflected lights are collected by the telescope. A PC controlled mechanism moves the primary mirror of the telescope to focus on a target. A 780 nm long-pass filter with a sharp cut-off is placed in front of the 200 μm diameter collection fiber for rejection of the Rayleigh scattered line. A pair of plano-convex lenses together with the long-pass filter are used to couple the received signals > 780 nm into the fiber which is then directed through a mechanical slit of 50 μm width into the spectrograph. The entire system is mounted atop a motorized altitude-azimuth fork, which is controlled by a handset. The cut-off wavenumber, dictated by the long-pass filter, is ~130 cm^{-1}. A 770 nm dichroic beamsplitter can be directly coupled to the rear port of the telescope to reflect light in the visible spectral range to a guide camera to remotely align the laser *in situ* and record the position at which the Raman measurement is taken. Since only the Stokes Raman signal is recorded, the dichroic would not affect the Raman measurements. The spectral resolution is ~9 cm^{-1} over the spectral range recorded with a 1200 lines/mm grating or ~15 cm^{-1} with a 500 lines/mm grating.

A mercury argon calibration light source (Ocean Optics HG-1) was used for wavelength calibration of the spectrograph. A second order polynomial was fitted to 10 known spectral lines between 790 and 870 nm, with a *rms* residual of ~0.03 nm, which translates to an uncertainty of ~0.5 cm^{-1} in Raman shift. The integration time was chosen to be such that the peak intensity is <80% of saturation and less than 15 mins so that the spectra are not overwhelmed by cosmic rays such that they can be removed by taking a median of 3 spectra. Shorter integration times and more repeat measurements are taken when there are significant variations in ambient light levels. Background subtraction was performed to remove the contribution from ambient light using the
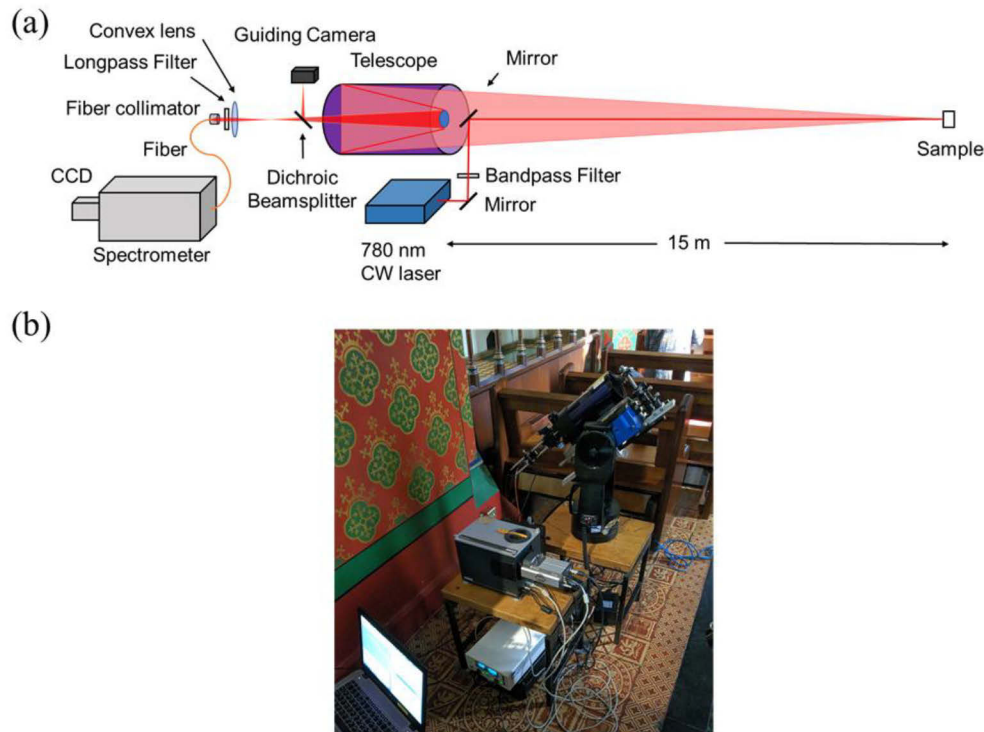
Fig. 1. Standoff Raman spectroscopy: (a) schematics of the standoff Raman instrument setup using a CW laser at 780 nm co-axial with the receiving optics; (b) the mobile system deployed *in situ* at the Blessed Sacrament Chapel in the Cathedral Church of St. Barnabas in Nottingham.

same integration time as the target spectrum but with the laser off. The background subtracted spectra were then corrected for the system spectral response by measuring the reflected spectrum of a Tungsten light source (Ocean Optics DH-2000, with a known continuous smooth spectrum) off a standard Spectralon white target. A baseline found by smoothing this spectrum using a moving median window of ~45 cm^{-1} was then subtracted from the spectral response corrected spectrum.

Almost all remote Raman systems use pulsed laser sources to maximize the laser intensity to increase the Raman signal and minimize daylight contribution for outdoor work. However, these systems are mostly used for the remote detection of minerals on planets, or for the safe detection from a distance, of minute quantities of explosives, where the effects of laser induced degradation are not the primary concern as long as the material is not burnt to lose their spectral signature [11].

In applications to cultural heritage, the effect of any laser induced degradation is to be avoided to comply with conservation ethics. Increased laser intensity increases the chances of laser induced degradation effects. For each material, there is an intensity threshold above which laser induced degradation effects occur. Recent studies have shown that high intensity pulsed lasers are damaging to all non-transparent materials from slightly scattering to slightly absorbing paint [14]. For some materials, the intensity damage threshold of pulsed lasers can be higher than that of a CW laser because pulsed lasers allow heat dissipation between pulses. However, for other materials such as red lead the damage threshold for CW and pulsed lasers are rather similar [14]. Overall, there is a trade-off between detection efficiency and laser induced degradation. Raman

intensity is proportional to the laser intensity and therefore the Raman signal S_{cw} induced by a CW laser is given by

$$S_{cw} \propto I_{cw}At_{cw} \tag{1}$$

where I_{cw} is the intensity of the CW laser, A is the area of the laser beam on the target (assume that the collection spot is matched to the excitation spot) and t_{cw} is the integration time. For a pulsed laser, the Raman signal S_P is given by

$$S_p \propto I_pAN_p\delta t \tag{2}$$

where I_P is the peak intensity of the pulsed laser, A is the area of the laser beam (or the collection area when matched) on the target, N_P is the number of pulses, δt is the pulse duration. The effective measurement time is then given by $t_p = \frac{N_p}{R}$, where R is the pulse repetition rate. The laser intensities need to be less than the damage threshold I_{th} For a pulsed laser, this translates to a pulse energy threshold of $\varepsilon_{th} = I_{th}A\delta t$, which effectively limits the maximum Raman signal achievable without degrading the material. For the same spot size on the target, to achieve the same Raman signal using a CW laser and a pulsed laser without causing laser induced degradation, the ratio of the measurement times is given by

$$\frac{t_{cw}}{t_p} = \frac{\varepsilon_{th}R}{P_{cw}} > R\delta t \tag{3}$$

where P_{cw} is the incident power of a CW laser on the target. Compared with a typical ns-pulsed laser with repetition rate of 10–100 Hz and pulse duration of ~5 ns, a CW laser can have a measurement advantage of up to 7 to 8 orders of magnitude in efficiency, if the damage threshold is comparable to the intensity of a typical CW laser in remote operation. For example, highly light sensitive pigments such as cochineal, orpiment and realgar will be in this category [12]. For a pigment of medium sensitivity to laser induced degradation such as red lead, the damage threshold of ~10^6 W cm^{-2} [13,14] means that the detection efficiency is about an order of magnitude lower for an ns-pulsed laser compared with a 50 mW CW laser assuming a spot size of a few mm in diameter. It is, therefore, better to use a CW laser in the remote Raman system for the investigation of historic wall paintings. The repetition rates of common ns-pulsed lasers are simply too low to ensure efficient Raman signal detection without elevating the power above the damage threshold. Including daylight subtraction procedure, the duty cycle of a CW laser Raman system is 50%, while the duty cycle of a 10–100 Hz ns-pulsed laser is 5×10^{-6} - 5×10^{-7}%.

A wavelength of 780 nm was chosen as a compromise on overall reduction in fluorescence in most materials of interest whilst having the benefits of a higher Raman efficiency and a lower cost Si CCD detector compared to the short wave infrared (SWIR) range (i.e. 1000–2500 nm).

3. Performance evaluation

3.1. Daylight subtraction

A big challenge for *in situ* Raman measurements for cultural heritage is the presence of variable ambient daylight during working hours. In buildings like churches and palaces where there are large windows without curtains, daylight cannot be avoided. Pulsed lasers at high peak power have been used to both boost their efficiency to make up for their low duty cycle and to make daylight contribution negligible in comparison to the high laser power through a gated detection synchronized to the laser pulse duration [15]. This cannot be applied to paintings as the high intensity would pose a threat to heritage objects. CW laser has also been applied for long range outdoor remote measurements, however the experiment was conducted at night to avoid daylight [16]. An automated online daylight subtraction program was developed in this project to address the issue of, on one hand, the need to lower the laser intensity to avoid damage whilst

maintaining a high Raman detection efficiency by using a CW laser, and on the other hand, the need to compensate for a variable background caused by daylight which can change dramatically in seconds. By modulating the laser beam on and off, the system can quickly respond to sunlight intensity changes (Fig. 2).
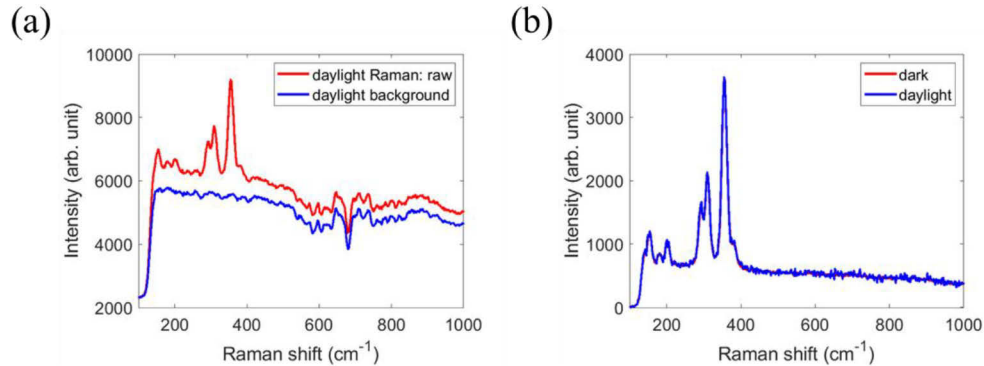

Fig. 2. Daylight subtraction spectra. (a) comparison between the measurements of an orpiment in animal glue sample at 3.3 m distance placed in front of the window using the standoff Raman system with the 780 nm CW laser on and off; the absorption bands correspond to H_2O absorptions from the atmosphere; (b) comparison of daylight subtracted Raman spectrum with that taken in total darkness.

3.2. Detection of common artist pigments

A collection of 53 common historic artist pigments were used to prepare reference paint samples in linseed oil, egg tempera or animal glue [17,18]. The pigment compositions were chemically analyzed with the main composition confirmed. Details of the analysis along with the pigment composition are given in [17]. The level of fluorescence between the different binding media are not significantly different probably because they are not as aged as those found in historic paints.

The 53 common pigments in various binding media were tested with the 780 nm standoff Raman. The standoff Raman setup was able to detect most pigments at 4 m within 1 min and nearly all of them within 30 min except for the copper pigments (e.g. most of the green pigments), the cadmium pigments, yellow ochres, most of the yellow organic pigments and most of the red organic pigments. Typical spectra of pigments with a range of Raman scattering efficiency are presented in Fig. 3.

With the exception of yellow ochre, yellow pigments are in general difficult to identify based on spectral reflectance alone [18]. The standoff Raman system has been successful in identifying nearly all the inorganic yellow pigments as well as the yellow organic pigment gamboge, therefore complementing remote spectral imaging analysis. For red pigments, vermilion, realgar, red lead, and chrome red are easily detectable as they are known to have strong Raman signals [19]. The only inorganic red pigment not detected was cadmium red. Most red and yellow organic pigments have low Raman scattering efficiency and their spectra are affected by fluorescence which increases the photon noise and hence reduces the signal to noise ratio [19,20]. Similarly, it is difficult to detect Raman signals from cadmium pigments because of the increased photon noise due to strong laser induced fluorescence of cadmium sulfide at this wavelength [21]. The intrinsic low Raman scattering efficiency and strong absorption at 780 nm of the copper pigments makes it difficult to detect them [19], despite the increase in Raman efficiency due to resonance.
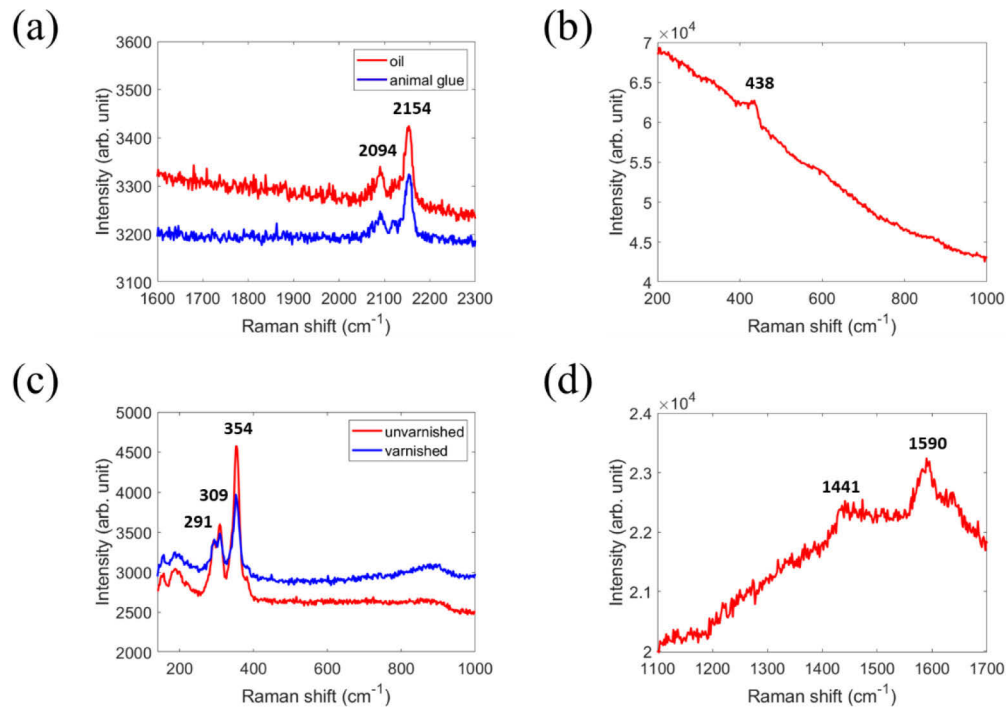
Fig. 3. Typical Raman spectra of pigments: (a) Prussian blue in animal glue and oil, integration time: 10 min; (b) zinc white in oil, integration time: 10 min; (c) orpiment in animal glue with and without varnish on top, integration time: 10 s; (d) gamboge in animal glue, integration time: 30 min.

4. Standoff in situ investigation of architectural interiors

The Cathedral Church of St. Barnabas in Nottingham is a fine example of Gothic Revival architecture in England. It was consecrated as a Church in 1844 and as a Cathedral in 1852. The architect was Augustus Welby Pugin (1812–1852), who also designed the decoration of the Houses of Parliament in London. Within the Cathedral, the Blessed Sacrament Chapel has been described as a "prayer book in stone". It is known that the Blessed Sacrament Chapel was restored in 1933 and 1974 [22]. However, how much work had been done in the original decoration or the later restoration remains unclear.

4.1. Complementary methods

The in-house developed standoff spectral system for automated scanning of wall paintings and architectural interiors, PRISMS [2], was used for the initial imaging of the murals. PRISMS images from 400–880 nm using a PC controlled filter wheel with 10 filters, where 9 filters are centered from 400 nm to 800 nm every 50 nm, each with a bandwidth of 40 nm, and one filter is centered at 880 nm with a bandwidth of 70 nm; a Jenoptik MF^{cool} CCD camera and a Meade ETX90 telescope. The system is placed on an alt-az telescope mount with PC controlled drives. Both focusing and scanning are automated. A Tungsten light with uniform projected illumination using a telescopic system was used for remote illumination.

An ASD LabSpec spectrometer (350–2500 nm) was used for high spectral resolution fiber optic reflectance spectroscopy measurements of the reference samples and for *in situ* measurements in the chapel at accessible heights to complement the remote measurements. The spectral resolution is 3 nm in the UV/VIS regime and 10 nm in the SWIR.

X-ray fluorescence spectroscopy (XRF): A handheld Niton XL3t XRF Analyzer was used for *in situ* measurements at accessible heights in the chapel to complement the reflectance spectroscopy and Raman measurements, since it measures the elemental content of the materials. It consists of an Au anode, with maximum voltage and current at 50 kV and 200 μA respectively. It is capable of detecting elements with atomic number $Z > 14$ without helium purge.

4.2. Analysis of painting materials

The SWIR reflectance spectra of various parts of the mural at accessible heights showed that the binding medium is consistent with oil because of the characteristic lines at ~2303 nm and ~2346 nm [23].

Different areas of the mural at various distances were studied from the same position on the ground using the standoff Raman system (Fig. 1(b)). The pigments used were the focus of our investigation since they could potentially reveal the time period when the paintings were created.

Figure 4 shows the data obtained from a red area of the mural. Firstly, reflectance spectra were acquired using the PRISMS remote spectral imaging system (Fig. 4(b)) which shows that the
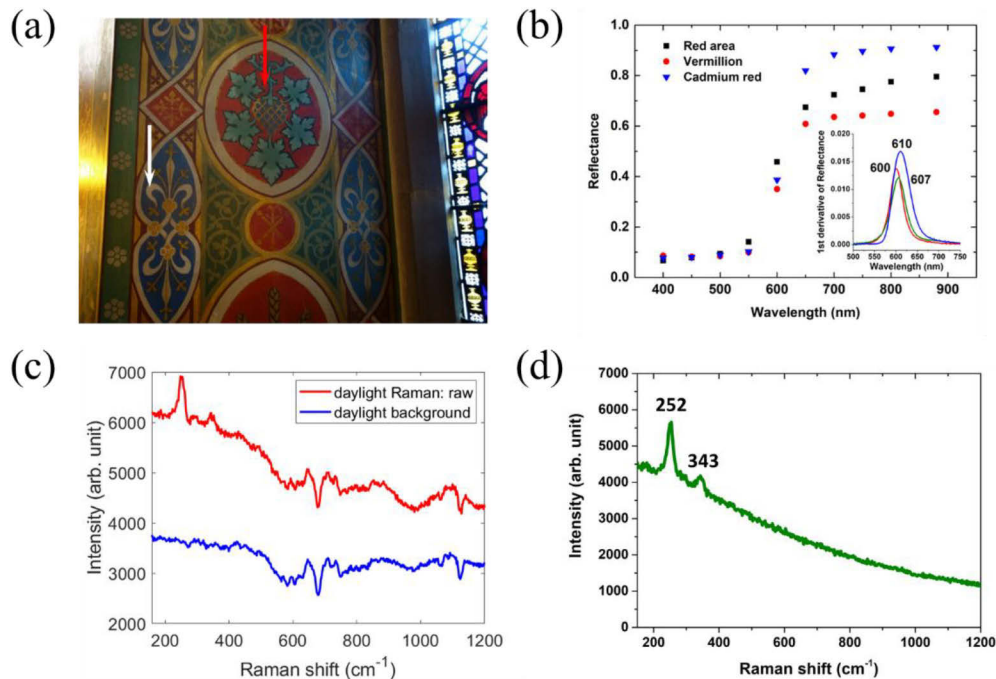

Fig. 4. Standoff investigation of a red area in the chapel: (a) color image of part of a mural next to a stained glass window (b) reflectance spectra collected with the remote spectral imaging system PRISMS of the red area (black filled squares) indicated by the red arrow in (a) compared with PRISMS spectra of a reference sample of vermilion (red dots) and cadmium red (blue triangle) oil paints; the inset shows the derivative of the reflectance spectra of cadmium red (peak at 610 nm), and two vermilion oil samples from two different sources (peaks at 600 nm and 607 nm); (c) the raw standoff Raman spectrum of the same red area (red), and the background spectrum collected over the same integration time with the laser off (blue) showing typical absorption bands of the solar spectrum (the band around 675 cm^{-1} corresponds to H$_2$O absorption lines ~823 nm from the atmosphere; the lines around 1056 and 1117 cm^{-1} corresponds to Ca II lines at ~850 and ~854 nm from the solar spectrum) ; (d) the processed spectrum after subtraction of daylight.

reflectance spectrum of the red region is similar to either vermilion or cadmium red. Vermilion was one of the most common red pigments until the 20th C when cadmium red, a less toxic synthetic pigment, became commercially available in 1919 [24]. Both pigments share similar reflectance spectral features that are within the natural variations due to particle size and trace impurity differences (Fig. 4(b)), which makes it impossible to distinguish between them solely by spectral reflectance. In red areas all over the chapel, such as the wall near the window (3.6 m), the wall behind the altar (11 m) and the central beam across the chapel (9.2 m), Raman signals characterizing vermilion were detected. Two strong peaks at 252 cm^{-1} and 343 cm^{-1} respectively, assigned to Hg–S stretching vibrational modes [20], were observed along with laser-induced fluorescence. It is worth noting that several absorption lines in the solar spectrum were recorded when measuring the red area near the stained glass window (Fig. 4(c)), which were fully removed after the subtraction of the ambient background. This is a good example that demonstrates the ability of this standoff Raman system to remotely detect and analyze pigments under the influence of daylight.

Portable XRF measurements of various areas at accessible height did not find cadmium and therefore no evidence for cadmium red and hence no evidence so far for post 1919 material on the mural.

Right next to one of the red areas near the window, a white area 4 m from the standoff Raman system was investigated (Fig. 4(a)). Again, reflectance spectroscopy cannot identify the white pigments. A weak peak at 991 ± 0.5 cm^{-1} was detected by the standoff Raman system (Fig. 5(a)) in the white area. This line can be attributed to the symmetric stretching mode (v_1) of the S–O bond in BaSO$_4$ [25]. It could be *constant white* (barium sulfate, BaSO$_4$) or *lithopone* (a mixture of barium sulfate and zinc sulfide, BaSO$_4$ and ZnS). Zinc sulfide is difficult to detect with Raman spectroscopy due to its low Raman efficiency [26]. The main peak of ZnS at 348 cm^{-1} was not detected in the lithopone reference sample. XRF measurements of various white areas at accessible heights found Ba, Zn and trace Pb (Fig. 5(b)), which would support the identification with lithopone. However, BaSO$_4$ is often used as a paint extender for zinc white (ZnO). Zinc white is a common white pigment used since the 19th century, and it is easily detectable by Raman spectroscopy with its main peak at 438 cm^{-1} (Fig. 3(b)), but this was not detected here. Therefore, the most likely identification of the white pigment is lithopone.
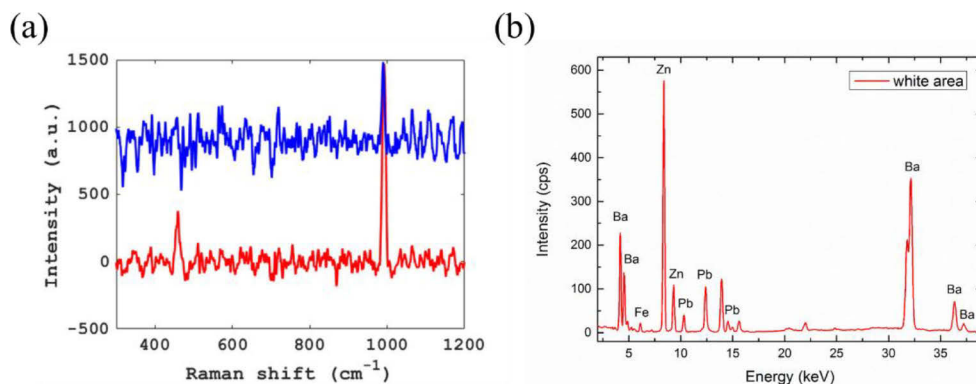

Fig. 5. Standoff investigation of a white area in the chapel (shown by the white arrow in Fig. 4(a)): (a) Standoff Raman measurement of a white area (blue) at a distance of 4 m compared with a sample of lithopone powder measured from the same distance in the lab (red); the baseline subtracted spectra are smoothed with a moving window of 6 cm^{-1}. (b) XRF measurement of a similar white area at accessible height.

Lithopone was manufactured on a commercial scale starting in 1874 (the year it was patented in England) but by the 1930s it was superseded by titanium white [27]. The detection of lithopone would suggest that the current painting scheme in the chapel was after the consecration of the church in 1844 but possibly before the 1933 restoration. There were records of alterations to the main parts of the cathedral made in the early 20th C but whether that included any alterations to the chapel is not known.

5. Conclusions

A standoff Raman spectroscopy system using a CW laser source at 780 nm is demonstrated to be able to operate from a distance of 3–15 m to identify most common historic artist pigments. The laser intensity of the standoff Raman system presented here is ~5 orders of magnitude lower than a micro-Raman system under standard operation for artworks. The risk of laser induced degradation is, therefore, negligible. The use of a CW laser presents significant advantages in measurement efficiency over a pulsed laser when it is paramount to operate at low laser intensity to ensure safe operation for all pigments.

The 780 nm standoff Raman system is shown to be able to operate under the influence of daylight through background subtraction by modulating the laser source through on/off cycles. Standoff Raman spectroscopy is demonstrated to complement our current visible/near infrared remote spectral imaging using PRISMS.

The standoff Raman system was successfully deployed in the Cathedral Church of St Barnabas in Nottingham to identify the pigments used in the Blessed Sacrament Chapel in order to date the painting scheme and hence verify its attribution to the celebrated architect Augustus Welby Pugin.

The application can be extended from murals to general architectural materials, such as stones, to determine the types of stones or to monitor the deterioration of buildings under the influence of the environment.

References

1. P. Vandenabeele, H. G. M. Edwards, and J. Jehlička, "The role of mobile instrumentation in novel applications of Raman spectroscopy: Archaeometry, geosciences, and forensics," Chem. Soc. Rev. **43**(8), 2628–2649 (2014).
2. H. Liang, A. Lucian, R. Lange, C. Cheung, and B. Su, "Remote spectral imaging with simultaneous extraction of 3D topography for historical wall paintings," ISPRS J. Photogramm. Remote Sens. **95**, 13–22 (2014).
3. S. P. Best, R. J. H. Clark, and R. Withnall, "Non-destructive pigment analysis of artefacts by Raman microscopy," Endeavour **16**(2), 66–73 (1992).
4. R. J. H. Clark, "Raman microscopy: application to the identification of pigments on medieval manuscripts," Chem. Soc. Rev. **24**(3), 187 (1995).

5. M. Pérez-Alonso, K. Castro, and J. M. Madariaga, "Investigation of degradation mechanisms by portable Raman spectroscopy and thermodynamic speciation: The wall painting of Santa María de Lemoniz (Basque Country, North of Spain)," Anal. Chim. Acta **571**(1), 121–128 (2006).
6. L. Bellot-Gurlet, F.-X. Le Bourdonnec, G. Poupeau, and S. Dubernet, "Raman micro-spectroscopy of western Mediterranean obsidian glass: one step towards provenance studies?" J. Raman Spectrosc. **35**(89), 671–677 (2004).
7. B. I. Łydzba-Kopczyńska, B. Gediga, J. Chojcan, and M. Sachanbiński, "Provenance investigations of amber jewelry excavated in Lower Silesia (Poland) and dated back to Early Iron Age," J. Raman Spectrosc. **43**(11), 1839–1844 (2012).
8. D. A. Leonard, "Observation of Raman scattering from the atmosphere using a pulsed nitrogen ultraviolet laser," Nature **216**(5111), 142–143 (1967).
9. J. Cooney, J. Orr, and C. Tomasetti, "Measurements separating the gaseous and aerosol components of laser atmospheric backscatter," Nature **224**(5224), 1098–1099 (1969).
10. S. M. Angel, N. R. Gomer, S. K. Sharma, C. McKay, and N. Ames, "Remote Raman spectroscopy for planetary exploration: A review," Appl. Spectrosc. **66**(2), 137–150 (2012).
11. A. Pettersson, I. Johansson, S. Wallin, M. Nordberg, and H. Östmark, ""Near real-time standoff detection of explosives in a realistic outdoor environment at 55 m distance," Propellants," Propellants, Explos., Pyrotech. **34**(4), 297–306 (2009).
12. H. Liang, R. Lange, A. Lucian, P. Hyndes, J. H. Townsend, and S. Hackney, "Development of portable microfading spectrometers for measurement of light sensitivity of materials. Paper 1612," in *Preprints, ICOM Committee for Conservation, ICOM-CC, 16th Triennial Conference, Lisbon* (2011), pp. 19–23.
13. L. Burgio, R. J. H. Clark, and S. Firth, "Raman spectroscopy as a means for the identification of plattnerite (PbO2), of lead pigments and of their degradation products," Analyst **126**(2), 222–227 (2001).
14. H. Liang, M. Mari, C. S. Cheung, S. Kogou, P. Johnson, and G. Filippidis, "Optical coherence tomography and non-linear microscopy for paintings – a study of the complementary capabilities and laser degradation effects," Opt. Express **25**(16), 19640 (2017).
15. S. K. Sharma, P. G. Lucey, M. Ghosh, H. W. Hubble, and K. A. Horton, "Stand-off Raman spectroscopic detection of minerals on planetary surfaces," Spectrochim. Acta, Part A **59**(10), 2391–2407 (2003).
16. R. L. Aggarwal, L. W. Farrar, and D. L. Polla, "Measurement of the absolute Raman scattering cross sections of sulfur and the standoff Raman detection of a 6-mm-thick sulfur specimen at 1500 m," J. Raman Spectrosc. **42**(3), 461–464 (2011).
17. H. Liang, R. Lange, B. Peric, and M. Spring, "Optimum spectral window for imaging of art with optical coherence tomography," Appl. Phys. B: Lasers Opt. **111**(4), 589–602 (2013).
18. S. Kogou, A. Lucian, S. Bellesia, L. Burgio, K. Bailey, C. Brooks, and H. Liang, "A holistic multimodal approach to the non-invasive analysis of watercolour paintings," Appl. Phys. A: Mater. Sci. Process. **121**(3), 999–1014 (2015).
19. L. Burgio and R. J. H. Clark, "Library of FT-Raman spectra of pigments, minerals, pigment media and varnishes, and supplement to existing library of Raman spectra of pigments with visible excitation," Spectrochim. Acta, Part A **57**(7), 1491–1521 (2001).
20. I. M. Bell, R. J. H. Clark, and P. J. Gibbs, "Raman spectroscopic library of natural and synthetic pigments (pre-≈ 1850 AD)," Spectrochim. Acta, Part A **53**(12), 2159–2179 (1997).
21. D. Anglos, M. Solomidou, I. Zergioti, V. Zafiropulos, T. G. Papazoglou, and C. Fotakis, "Laser-Induced Fluorescence in Artwork Diagnostics: An Application in Pigment Analysis," Appl. Spectrosc. **50**(10), 1331–1334 (1996).
22. M. M. Cummins, *Nottingham Cathedral - a History of Catholic Nottingham* (1985).
23. M. Vagnini, C. Miliani, L. Cartechini, P. Rocchi, B. G. Brunetti, and A. Sgamellotti, "FT-NIR spectroscopy for non-invasive identification of natural polymers and resins in easel paintings," Anal. Bioanal. Chem. **395**(7), 2107–2118 (2009).
24. M. de Keijzer, "The history of modern synthetic inorganic and organic artists' pigments," Contrib. to Conserv. Res. Conserv. Netherlands Inst. Cult. Herit., 42–54 (2002).
25. P.-L. Lee, E. Huang, and S.-C. Yu, "High-pressure Raman and X-ray studies of barite, BaSO4," High Pressure Res. **23**(4), 439–450 (2003).
26. A. Fairbrother, V. Izquierdo-Roca, X. Fontané, M. Ibáñez, A. Cabot, E. Saucedo, and A. Pérez-Rodríguez, "ZnS grain size effects on near-resonant Raman scattering: optical non-destructive grain size estimation," CrystEngComm **16**(20), 4120 (2014).
27. R. Capua, "The Obscure History of a Ubiquitous Pigment: Phosphorescent Lithopone and Its Appearance on Drawings By John La Farge," J. Am. Inst. Conserv. **53**(2), 75–88 (2014).